State-to-State Rate Constant Calculations for V−V Energy Transfer in CO−N_2 Collisions

A. Kurnosov,[†] M. Cacciatore,*[,‡] and G. D. Billing[§]

Troitsk Institute of Innovation and Fusion Research, 142092 Troitsk, Moscow Region, Russia, CNR−IMIP, c/o Department of Chemistry, University of Bari, via Orabona N°4, 70126 Bari, Italy, and Department of Chemistry, H.C.Ørsted Institute, University of Copenhagen, DK-2100 Ø, Copenhagen, Denmark

Received: August 7, 2002; In Final Form: January 30, 2003

Single and multiquantum vibrational relaxation of low and highly vibrationally excited levels of CO in collisions with N_2 is studied within the semiclassical coupled state method. The dynamics is followed using ab initio interaction potential for the short-range interaction and updated multipole expansions for the long range interaction. Compared to the previous study, a better agreement with the available experimental rate constants is obtained, particularly in the critical low temperature regime down to $T = 80$ K. Remarkable corrections are found for rate constants for single and multiquantum transitions between highly excited CO and N_2 molecules.

1. Introduction

We are in this work concerned with the vibrational quantum exchanges in collisions between CO and N_2 molecules:

$$N_2(v = 1) + CO(v') \rightarrow N_2\,(v = 0) + CO(v' + 1) \quad (1)$$

$$N_2(v) + CO(v') \rightarrow N_2(v - \Delta v) + CO(v' + \Delta v'), \quad \Delta v = 1, 2;\ \Delta v' = 1, 2, 3 \quad (2)$$

These collisional processes are of great importance in many research areas of fundamental and technological interest such as for the N_2−CO laboratory plasmas under nonthermal equilibrium conditions, in the chemistry of the upper atmosphere, in aerothermodynamics, etc. Theoretical attempts to characterize and, eventually, to implement chemical processes connected to the nonequilibrium vibrational relaxation of CO and N_2 requires the write up and solution of the kinetic equations for each level of the vibrational manifold of the two molecules. This, in turn, implies the knowledge of a large set of accurate state-to-state rate constants for one quantum and multiquantum V−V and V−T/R energy exchanges. Recent experimental results have shown the necessity in new kinetic information about energy transfer processes with highly excited CO molecules. In particular, a rather strong influence was found[1] of small additions of N_2 into the CO:He active medium on the spectral characteristics of the first overtone CO laser for transitions with $\lambda > 3.8$ mm. This phenomenon could be explained by quasi-resonance multiquantum asymmetric V−V processes:

$N_2(v = 0) + CO(v') \rightarrow N_2\,(v = 1) + CO(v' - 2)$ (reverse to processes 2), but no information about such processes for $v >$ 30 is available.

For the CO−N_2 system, the only available sets of V−V and V−T rate constants, which has been largely used in kinetic modeling, are those calculated in ref 2 and in the classical work of Billing.[3] These sets of rates are, however, incomplete particularly with respect to the processes 2. In addition to that, the approximations made in the collisional model used in these studies could affect the accuracy of the multiquantum transition rates among the vibrationally excited states in CO, i.e., for transitions that could play an important role in the relaxation kinetics of CO.

Therefore, the primary aim of this work is to improve the accuracy of the rate constants for processes 1 and 2 by removing some of the approximations made in the previous studies.[2,3] The analogous revision of results for another pair of diatomics, CO−CO, was recently done.[4−6] We first make use of an improved ab initio interaction potential for N_2−CO which is different with respect to the one previously used both in the repulsive and the attractive part of the interactions. Second, we remove the energy corrected harmonic oscillator approximation made in the previous collisional model developing a multistate expansion of the total vibrational wave function over a convergent set of Morse wave functions of the two separated molecules.[7] This gives a proper description for the multiqantum transitions that are sensitive to a correct description of the vibrational anharmonicity. It will be shown that the agreement between the theoretical and the experimental rate constants for the transition $K(1,0|0,1)$ is much better than that reached with the previous studies for a wide range of temperatures, particularly in the region of low and thermal temperatures $80 < T < 400$ K. The second objective of the present study is the calculation of rate constants for a sample of asymmetric multiquantum processes responsible for V−V transfers from high vibrationally excited states of CO to low levels of N_2.

2. Interaction Potential

We construct the N_2−CO potential as a sum of short-range (SR) repulsive potential with the long-range (LR) multipole interactions. Thus, we have

$$V_{N_2-CO}(R,r_i,\gamma_i,\varphi_i) = V_{S-R} + V_{L-R} \quad (3)$$

where R is the center of mass distance between the two molecules, r_i is the intramolecular vibrational distance in

* To whom correspondence should be addressed. E-mail: cacciatore@area.ba.cnr.it. Fax: +39-080-5442024.
† Troitsk Institute of Innovation and Fusion Research.
‡ University of Bari.
§ University of Copenhagen.

10.1021/jp0218239 CCC: $25.00
Published on Web 03/13/2003

molecule i ($i = 1,2$), and γ_i and φ_i are the spherical polar angles which define the in-plane and out-of-plane rotations of the two molecules in a coordinate system having the Z axis along the R axis. Because any ab initio potential for the N_2-CO interaction has not yet been calculated, we assume as reference potential for the short-range interactions the interaction potential proposed by Ling and Rigby[8] for the isoelectronic N_2-N_2 system.

Therefore, we express the S−R potential as a sum of exponentially repulsive atom−atom interactions:

$$V_{S-R} = \sum_{i=1}^{4} A \exp[-R_i(\alpha_0 + \alpha_1 R_i)] \quad (4)$$

where it is assumed that the interaction between N and C is identical to the N−O interaction. R_i is the N−C (N−O) separation distance.

As usual, we express the long-range potential as a sum of dipole−quadrupole, quadrupole−quadrupole and dispersion interactions:

$$V_{L-R} = V_{D-Q} + V_{Q-Q} + V_{disp} \quad (5)$$

where the quadrupole-quadrupole interaction term is given by the following equation:[28]

$$V_{Q-Q} = \frac{3}{4}\Theta_1\Theta_2\frac{1}{R^5}[1 - 5\cos^2\gamma_1 - 5\cos^2\gamma_2 - 15\cos^2\gamma_1\cos^2\gamma_2 + 2(\sin\gamma_1\sin\varphi_1\sin\gamma_2\sin\varphi_2 + \sin\gamma_1\cos\varphi_1\sin\gamma_2\cos\varphi_2 - 4\cos\gamma_1\cos\gamma_2)^2] \quad (6)$$

here Θ_i is the quadrupole moment of the oscillator i.

The usual expansion of the quadrupole moment around the equilibrium intramolecular distance $\bar{r}_i$ of the oscillator is assumed

$$\Theta = \Theta_0 + \Theta_1(r_i - \bar{r}_i) + \Theta_2(r_i - \bar{r}_i)^2 \quad (7)$$

The factors in the quadrupole expansion of CO are taken from Billingsley and Krauss,[9] whereas the quadrupole moment components of N_2, Θ_0, and Θ_1, correspond to the values given by Buckingham et al.[10] and Reuter and Jennings,[11] respectively.

A five-term expansion has been assumed for the dipole moment of CO

$$\mu = \sum_{i=0,4}\mu_i(r - \bar{r})^i \quad (8)$$

The dipole parameters are determined by fitting this expression to the dipole moment function of CO recently discussed and recalculated by Langhoff et al.[12] Compared to the previously used dipole moments[3] based on the Yong and Eachus[13] recommended values, the Langhoff dipole function exhibits a maximum at larger bond distance of CO such that in the region of $r > 1.6$ Å the dipole moment is much larger and positive (see Figure 1). Because the effective bond distance of CO is larger for excited molecules, the different behaviors of the dipole moment in the expanded r region could have an impact on the relaxation of the highly excited vibrational levels of the diatom.

The dipole−quadrupole interaction term is given in the usual way as

$$V_{D-Q} = \frac{3}{2}\mu\,\Theta\frac{1}{R^4}[\cos\gamma_1(3\cos^2\gamma_2 - 1) - 2\cos\gamma_2 (\sin\gamma_1\sin\varphi_1\sin\gamma_2\sin\varphi_2 + \sin\gamma_1\cos\varphi_1\sin\gamma_2\cos\varphi_2)] \quad (9)$$

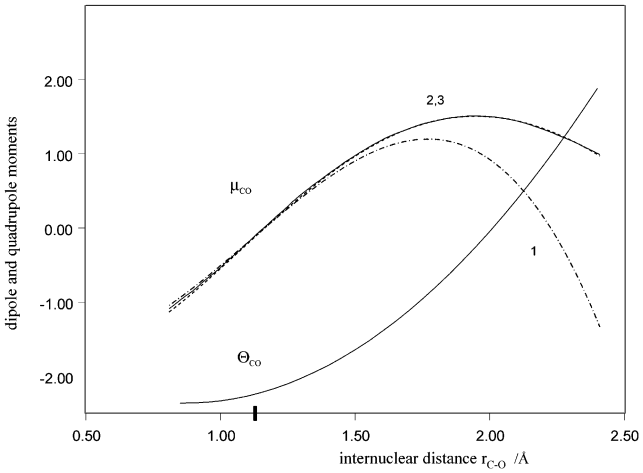

Figure 1. Electric dipole moment function of CO, μ_{CO} in units of D, is shown as a function of the internuclear distance r_{CO}. Curve 1: data from ref 13. Curve 2 (solid line): ab initio data from ref 12. Curve 3 (dotted line): analytic fit to the data of ref 12. The quadrupole moment function Θ_{CO} (in units of E) is also shown by the lowest solid line. The bold tick on the X axis shows the equilibrium distance of CO.

TABLE 1: Potential Parameters Used in eqs 4, 7, 8, and 10

parameters	Pot I	Pot II	Pot III
A/eV	614.11[a]	517.12[d]	517.12
α_0/ Å^{-1}	2.2412[a]	3.60[d]	3.60
α_1/ Å^{-2}	0.321[a]	0.	0.
C_6/ eV Å^{-6}	48.205[b]	48.205	48.205
μ_0(CO)/ D	−0.122227[c]	−0.112[e]	−0.122227
μ_1(CO)/ D Å^{-1}	3.305[c]	3.118[e]	3.305
μ_2(CO)/ D Å^{-2}	0.050 [c]	−0.150[e]	0.050
μ_3(CO)/ D Å^{-3}	−2.715[c]	−2.360[e]	−2.715
μ_4(CO)/ D Å^{-4}	0.9915[c]	0.	0.9915
Θ_0(CO)/ E	−2.241[f]	−2.241	−2.241
Θ_1(CO)/ E Å^{-1}	0.935[f]	0.935	0.935
Θ_2(CO)/ E Å^{-2}	1.814[f]	1.814	1.814
$\Theta_0(N_2)$/ E	−1.526[g]	−1.635[f]	−1.526
$\Theta_1(N_2)$/ E Å^{-1}	2.371[h]	1.720[f]	2.371
R_{min}/ Å	4.34	3.85	3.85
V_{min}/meV	−4.90	−8.15	−8.15

[a] Reference 8. [b] Reference 14. [c] Analytical fit (see eq 8) to the data of reference 12. [d] Reference 3. [e] Reference 13. [f] Reference 9. [g] Reference 10. [h] Reference 11. 1D = 10^{-18} esu cm; 1E = 10^{-26} esu cm^2.

Finally, the dispersion term used in eq 5 is the R^{-6} term assumed in the previous calculations[2,3]

$$V_{disp} = -\frac{1}{2}\frac{C_6}{R^6} \quad (10)$$

The parameters of the interaction potential appearing in eqs 4, 7, 8, and 10 are given in the second column of Table 1.

The choice of the SR potential parameters appearing in eq 4 is very critical because the collisional coefficients for V−V and V−T energy transfer are sensitive particularly to the short range interactions, and indeed, the accuracy of the calculated vibrational transition probabilities relies mostly on the accuracy with which V_{S-R} is known. Furthermore, the long range interactions can also have, as demonstrated in several works, an impact on the excitation amplitudes for resonant or near-resonant transitions, particularly at low impact energies. Therefore, to test the sensitivity of the rates upon both the potential surface behaviors and the collisional method, we have performed different calculations assuming three different surfaces. In Table 1, Pot I is the new surface constructed in the present work as described above, Pot II is the semiempirical best-fitted potential obtained

by Billing,[3] and Pot III is constructed as sum of the V_{S-R} assumed in Pot II with the updated long-range coefficients assumed in Pot I. The position (R_{min}) and the value (V_{min}) of the potential well of the angle averaged Pot I−III are given in Table 1.

3. Collisional Method

Calculations of the rate constants for processes 1 and 2 have been carried out on the model interaction potential described in the previous section using the time-dependent coupled state semiclassical method.[7,15] This collisional method, described in many papers, has been successfully applied to describe multiquantum vibrational energy exchanges for numerous atom/diatom and diatom/diatom collisional systems. Therefore, only a brief description of the model is given here. According to this method, the vibrational motion of the two colliding molecules is described quantum-mechanically, whereas the nuclear motion for the molecular translations and molecular rotations is treated classically by solving the corresponding equations of motion of two rigid rotors in an effective Hamiltonian H_{eff}

$$H_{eff} = \frac{1}{2\mu}(P_x^2 + P_y^2 + P_z^2) + \sum_i \frac{1}{2m_i}(p_{x_i}^2 + p_{y_i}^2 + p_{z_i}^2) + \sum_i \lambda_i(r_i^2 - \bar{r}_i^2) + V_{eff}(R(t), r_i, \{\Omega\}) \quad (11)$$

where P_x is the x component of the momentum for the relative motion and p_{x_i} is the x component of the momentum of molecule i. $\{\Omega\}$ is again the set of angles (γ_i, φ_i) for r_i, and λ_i are the Lagrange multipliers. V_{eff} is the Ehrenfest average potential which couples the dynamics of the two quantum oscillators with the propagation of the classical trajectory $R(t)$, and it is given as the expectation value of the interaction potential, V_{N2-CO}, over the quantum vibrational coordinates

$$V_{eff} = \langle \Psi(t) | V(R(t), r_i, \{\Omega\}) | \Psi(t) \rangle \quad (12)$$

V_{eff} is then obtained by expanding the total wave function of the quantum degrees of freedom, $\Psi(t)$, in rotationally distorted Morse product wave functions of the two unperturbed oscillators $\Phi_{n_1}\Phi_{n_2}$

$$\Psi(r_1, r_2, t) = \sum_{n_1, n_2} \Phi_{n_1}(r_1, t)\Phi_{n_2}(r_2, t) \exp\left[\frac{1}{\hbar}(E_{n_1} + E_{n_2})\, t\right] a_{n_1 n_2}(t) \quad (13)$$

where

$$\Phi_{ni}(r_i, t) = \Phi_{n_i}^{\,0}(r_i) + \sum_{m_i \neq n_i} \Phi_{m_i}^{\,0}(r_i) \frac{H_{m_i n_i}}{E_{n_i}^{\,0} - E_{m_i}^{\,0}} \quad (14)$$

and

$$H_{m_i n_i} = -\, j_i^2(t) m_i^{-1} (\bar{r}_i)^{-3} \langle \Phi_{m_i}^{\,0} | r_i - \bar{r}_i | \Phi_{n_i}^{\,0} \rangle \quad (15)$$

$\Phi_{n_i}^{\,0}$ and $E_{n_i}^{\,0}$ are the eigenfunctions and the eigenvalues for the Morse oscillators. The second term in eq 14 is the first-order centrifugal stretching term which couples the rotational to the vibrational motion of the diatom, and j_i is the rotational momentum of molecule i. The effective potential is finally obtained by expanding the interaction potential V to the second order in the bond displacement of the two molecular oscillators.[7,15]

In eq 13, $a_{n_1 n_2}(t)$ are the amplitudes for vibrational transitions and E_{n_i} are the eigenvalues for the Morse functions corrected by the Coriolis coupling elements $H_{m_i n_i}$. Inserting the expansion 13 in the time-dependent Schrödinger equations yields a set of coupled equations for the vibrational amplitudes. These equations are solved simultaneously with the classical Hamilton's equations for the relative translational and the rotational motion of the two molecules in the effective potential $H_{eff}(t)$.

The total semiclassical cross section for the vibrational transition ($n_1, n_2 \rightarrow n_1', n_2'$) is then obtained from the computed quantum amplitudes by Monte Carlo averaging over the action-angle variables specifying the rotational and translational initial conditions of the classical trajectory

$$\sigma_{n_1 n_2 \rightarrow n_1' n_2'}(U) = \frac{\pi\hbar^6}{8\mu I_1 I_2 (kT_0)^3} \int_0^{l_{max}} \mathrm{d}l \int_0^{j_{1max}} \mathrm{d}j_1 \int_0^{j_{2max}} \mathrm{d}j_2 \, (2j_1 + 1)(2j_2 + 1)(2l + 1) \frac{1}{N_t} \sum |a_{n_1 n_2 \rightarrow n_1' n_2'}|^2 \quad (16)$$

where μ and I_i are, respectively, the reduced mass of the relative motion and the moment of inertia of molecule i and l is the orbital angular momentum. U is the classical part of the energy, $U = E_{kin} + E_{rot}^1 + E_{rot}^2$, where E_{kin} is the impact kinetic energy and E_{rot}^i is the rotational energy of molecule i. N_t is the total number of trajectories. T_0 is an arbitrary reference temperature included in order to give the cross section the correct unit.

The cross sections for any transition examined in this work have been calculated at 19 values of the initial energy U from 50 cm^{-1} up to 25 000cm^{-1}. Usually the number of classical trajectories calculated at each energy is $N_t = 1000$, and this gives a numerical accuracy of about 10−15% on the computed rate constants. For energy below 6000 cm^{-1}, the number of coupled Schrödinger equations to solve is 120, whereas at the higher energies, the number of coupled vibrational eigenstates is larger so that up to 140 equations of motion for the vibrational dynamics were solved.

The state-to-state rate constants are then obtained by averaging over an initial Boltzmann distribution of kinetic and rotational energies

$$K_{n_1 n_2 \rightarrow n_1' n_2'}(T) = \sqrt{\frac{8kT}{\mu\pi}} \left(\frac{T_0}{T}\right)^3 \int_{\epsilon_{min}}^{\infty} \sigma_{n_1 n_2 \rightarrow n_1' n_2'}(U) \exp\left(-\frac{\bar{U}}{kT}\right) \mathrm{d}\left(\frac{\bar{U}}{kT}\right) \quad (17)$$

where $\bar{U}$ is now the symmetrized effective energy[15]

$$\bar{U} = \frac{1}{2}\left\{U - \frac{1}{2}\Delta E + [U(U - E)]^{1/2}\right\}$$

E is the total energy and $\Delta E = E_{n_1'} + E_{n_2'} - E_{n_1} - E_{n_2}$.

4. Results

As one of the main objects of this work and as a good test for the used intermolecular potential, the rate constants for the endothermic process

$$N_2(v = 0) + CO(v' = 1) \rightarrow N_2(v = 1) + CO(v' = 0) \quad (18)$$

are calculated using the semiclassical coupled state expansion with the new ab initio potential surface constructed as described

TABLE 2: Higher Order Dispersion and Multipole Expansion Terms of Eq 19

C_6/ eV Å^6	C_8/ eVÅ^8	C_{10}/ eVÅ^{10}	Φ(CO)/ (eVÅ^7)$^{1/2}$	Φ(N_2)/ (eVÅ^7)$^{1/2}$
49.0[a]	483.91[a]	4788.4[a]	−2.12[b]	−2.84[c]
			−5.226[d]	−3.877[d]

[a] Reference 18. [b] Reference 19. [c] Reference 20. [d] Reference 21.

TABLE 3: Endothermic Rate Constants for the Process $N_2(v = 0) + CO(v' = 1) \rightarrow N_2(v = 1) + CO(v' = 0)$

T/K	expt ref 16	Pot I	Pot II	Pot III	Pot II (ref 3)
100	2.95(−16)[a]	2.53(−16)	1.10(−15)	1.60(−15)	3.58(−16)
200	2.22(−15)	2.33(−15)	4.60(−15)	7.10(−15)	2.03(−15)
300	5.52(−15)	6.35(−15)	9.13(−15)	1.45(−14)	8.30(−15)
500		1.59(−14)	1.84(−14)	2.89(−14)	1.44(−14)
1000		3.81(−14)	4.08(−14)	5.89(−14)	3.32(−14)
2000		8.55(−14)	8.64(−14)	1.11(−13)	8.70(−14)
3000		1.36(−13)	1.33(−13)	1.59(−13)	1.83(−13)

[a] 2.95(−16) = 2.95 × 10^{-16}.

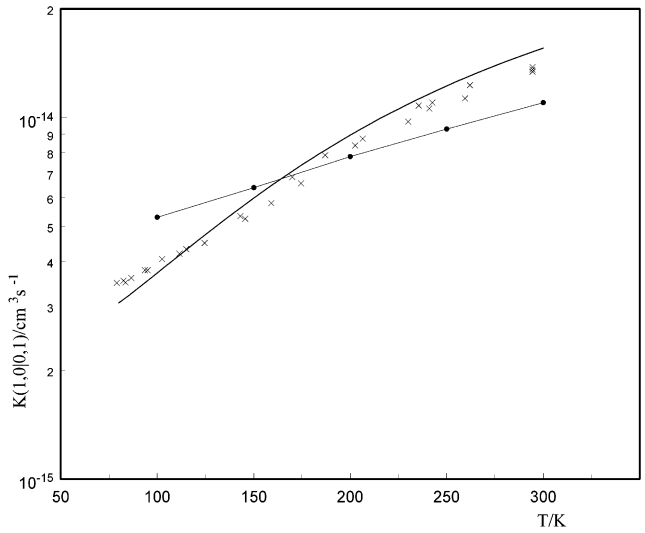

Figure 2. Exothermic rate constants for the process $N_2(v = 1) + CO(v' = 0) \rightarrow N_2(v = 0) + CO(v' = 1)$ reported as a function of the gas temperature. The results obtained in this work are shown by the solid line. The rates calculated by Billing [3] are given by (●), and the experimental rates[16] are shown by (×).

in section 2 with the corresponding parameters given in Table 1 (Pot I). Because the experimental data of Allen and Simpson,[16] assumed as the reference data to the calculated rates, were accurately determined we have undertaken special efforts to minimize the possible dispersion of the rate constant values. Therefore, the total number of classical trajectories for each energy was increased to more than 10 times, such that the achieved accuracy for the rate constants of the process 18 was better than 2%. This statistical uncertainty is applicable to all of the new rate constants calculated for this transition reported in Figures 2−5 and in Table 3. It is worth noticing that the numerical uncertainty of the old data[2,3] was estimated around 20−30%.

In Figure 2, the semiclassical rate constants $K(1,0|0,1)$ for the process 18 in the exothermic direction are reported at different temperatures in the range $T = 79-294.5$ K together with the experimental rates.[16] From the reported data, it is easily seen that the agreement of our results with the experimental ones is very good, being better than 10% in the full temperature range. The comparison with results of previous semiclassical calculations[3] is also shown in Figure 2. It is found that the current results agree with the experimental data better than the previous ones, particularly in the low temperature region. As it will be confirmed later, the better agreement of the new rate constants with the experimental data is mostly due to the new interaction potential and collisional method assumed in the calculations, rather than to the improved numerical accuracy.

In the low-temperature regime, the V−V (and V−T) energy exchange mechanism is quite complex. In particular, at low impact energies, the Coriolis coupling between the vibrational and the rotational motion of the colliding molecules can play a relevant role. This dynamical behavior, and the associated molecular orbiting effect, is of minor importance in the high-temperature regime. In the semiclassical coupled-state method, the molecular rotations and the V−R coupling term are appropriately considered in the scattering equations.

To better describe the collisional dynamics in this critical temperature regime, we have tried to point out the effect of the higher order attraction terms in the V_{L-R} interaction potential of eq 5, that is, the dispersion terms C_6, C_8, and C_{10} and the quadrupole−octopole and dipole−octopole Coulomb interactions

$$V_{LR}^{(1)} = V_{LR} + V_{\mu-\Phi} + V_{\theta-\Phi} - f_6(R)C_6R^{-6} - f_8(R)C_8R^{-8} - f_{10}(R)C_{10}R^{-10} \quad (19)$$

The inclusion of these additional terms to the "base" PotI implies the use of an appropriate damping function $f_n(R)$ which however cannot be unequivocally defined. We have in our case assumed for the damping function the functional form proposed by Tang and Toennies[17]

$$f_n(R) = 1 - \left[\sum_{k=0}^{n} \frac{(\alpha R)^k}{k!}\right] \exp(-\alpha R) \quad (20)$$

We take $\alpha = 2.24$ Å^{-1}, that is, the effective value of the α_i parameters used in the SR potential, whereas for the dispersion terms, we assume the values proposed by Rijks and Wormer.[18] Because different values have been proposed for the octopole moments of N_2 and CO, we have also tested two different values of the octopole moments taken from refs 19 and 20 and from ref 21, respectively. Table 2 reports the higher order attractive coefficients assumed in the extended LR potential given by the eq 19.

The newly obtained results are shown in Figure 3. Here the rate constants $K(0,1|1,0)$ obtained from the base Pot I are reported together with the expanded LR potential of eq 19 and assuming the two different sets of the octopole moments for N_2 and CO reported in Table 2. The reported experimental data are from Allen et al.[16] and Mastrocinque et al.[22] We notice that the inclusion of the higher order terms in the V_{LR} potential has a large impact on the rate constants in the low temperature regime, being practically negligible at temperatures larger than 300 K above which there is a substantial convergence between the rates obtained with and without the higher order V_{LR} terms. At low *T*, the higher multipole terms have a too large an effect, such that the corresponding rate constants are largely overestimated and in strong disagreement with the corresponding experimental rates. Moreover, the inclusion of these terms has another effect on the vibrational energy transfer process, that is, the appearance of a small temperature reversal at around $T = 120$ K, more pronounced when the Spelsberg's octopole values[21] are used: this effect is not supported from the available experimental results. Therefore, the results shown in Figure 3 demonstrate that, within the assumed parameters of eqs 4, 5, and 20, the base potential surface I is the most reliable potential

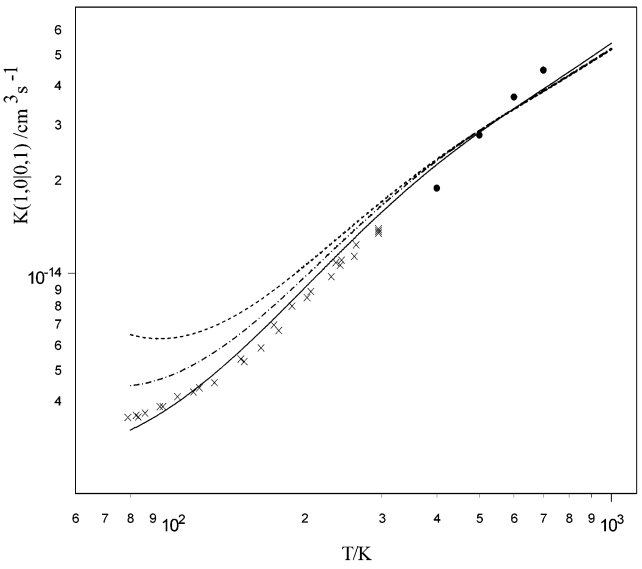

Figure 3. Rate constant $K(1,0|0,1)$ calculated using the "base" potential energy surface Pot I (solid line), the extended Pot I with the octopole moments of Spelsberg et al.[21] (upper dashed line), and the extended Pot I with octopole moments given in refs 19 and 20 (dot−dashed). The experimental data are from refs 16 (×) and 22 (●).

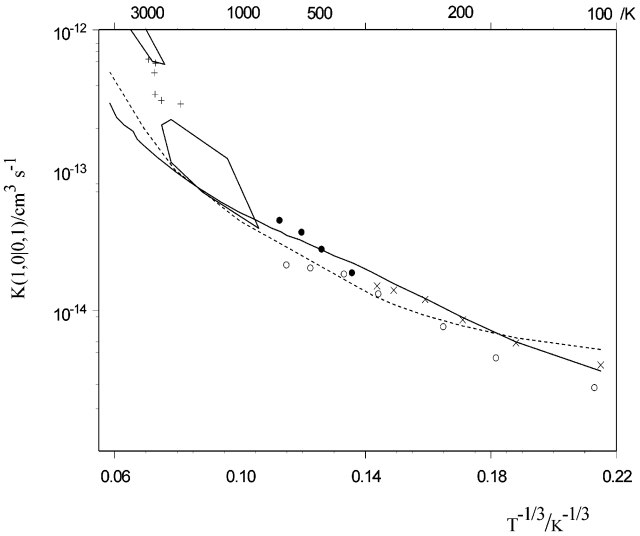

Figure 4. Landau−Teller plot of the exothermic rate constant for the process $N2(v = 1) + CO(v' = 0) \rightarrow N_2(v = 0) + CO(v' = 1)$. The solid line shows our results, and the dashed line are the rate calculated in ref 3. Experimental data are indicated by (×) ref 16, (○) ref 23, (●) ref 22, and (+) ref 25; closed area from 1000 to 2000 K from ref 24, closed area in the upper left corner of the plot shows the high-temperature data from ref 26.

to describe the V−V energy exchange mechanism for process 1. It is worth noticing that, as discussed in several works, the effect of the higher order multipoles on the rate constants depends much upon the choice of the damping function so that the definition of the effective role played by these attractive forces would require further investigations with different α values and different functionals for $f_n(R)$.

The behavior of the rate constants in a larger temperature range is shown in Figure 4 where the exothermic rate constants $K(1,0|0,1)$ obtained using Pot I are reported in the Landau−Teller plot together with the available experimental results.[16,22−26] The good agreement with experiments is really reached up to $T = 2000$ K, but in the high temperature regime, between $T = 2000$ K and $T = 4000$ K, the new semiclassical rates still remain below the shock tube data by a factor about 4. Such discrepancies, rather than to the collisional method, are most likely due to some inadequacy of the interaction potential, namely, the short-range repulsive part. This is a further evidence that the same set of parameters in the SR part of the interaction potential (A, α_0, α_1) can hardly be capable of correct description of collision dynamics in a large energy range, from sub to thermal collisional energies ($5 \times 10^{-3} - 1$ eV).

To investigate whether the excellent agreement between the new rate constants and the experimental data reached in this work in an ample temperature range, $T = 79-2000$ K, is due to the new potential surface or to the collisional method, we have performed additional calculations of the rate constants using the potential surface determined in ref 3 (Pot II of Table 1) but within the coupled state expansion method. The corresponding results are reported in column 4 of Table 3. We notice that the use of the intermolecular potential Pot II overestimates the rate constants (up to a factor larger than 4 at $T = 100$ K), but at temperatures higher than $T = 500$ K, there is a substantial convergency between the two sets of rates. Because of the near-resonant character of process 18, the corresponding energy mismatch is $\Delta E = -187.33$ cm^{-1}, these large discrepancies can be due to both the different long range and short range interactions assumed in the two surfaces. To check the relative importance of the SR and the LR forces, we have recalculated the rate constant $K(1,0|0,1)$ using Pot III. We recall that Pots III and II have the same SR potential but different LR interactions. Inspection of the data reported in Table 3 in columns 4 and 5 shows that a substantial agreement exists between the rates obtained with Pots III and II thus proving that, although the interferences between the long range and short range forces cannot certainly be discarded, the short-range part of the potential is the most effective one even for near-resonant vibrational energy transfer in a ample range of collisional temperatures. Obviously, the same conclusion holds when comparing the rate constants obtained using Pots I and III: here a large discrepancy is observed between the corresponding rate constants as a result of the different SR part of the interaction potential.

For the sake of completeness, we have in column 6 of Table 3 reported the semiclassical rates calculated with the harmonic oscillator approximation.[3] By comparing these rates with those calculated using the same Pot II but with the coupled state expansion (column four of the same Table 3), the discrepancies associated to the two different collisional methods can be pointed out. The same behavior has been found for the CO−CO system.[4,6] We also note that the old data obtained by Billing[3] are better than the new results with Pot II and in substantial agreement with the new rate constants obtained using Pot I. In fact, the old rate constants were obtained in a semimpirical way by changing the parameters of the SR potential until a good agreement was reached between the calculated and the experimental data. This is the reason the old data remain close to the new ab initio rates. Nevertheless, the old rate constants are less accurate, in the low temperature regime, as clearly shown in Figures 2 and 4.

We now focus on the vibrational energy transfer involving the low-lying vibrational levels of CO for the processes

$$N_2(v = 1) + CO(v' - 1) \rightarrow N_2(v = 0) + CO(v') \quad (21)$$

In Figure 5, the corresponding rate constants calculated using Pot I at $T = 300$ K are reported as a function of the vibrational quantum number v', v' in the interval $1 \div 14$. The comparison with the experimental data of Hancock and Smith[27] is not as good as the agreement reached for the transition (1,0|0,1). In

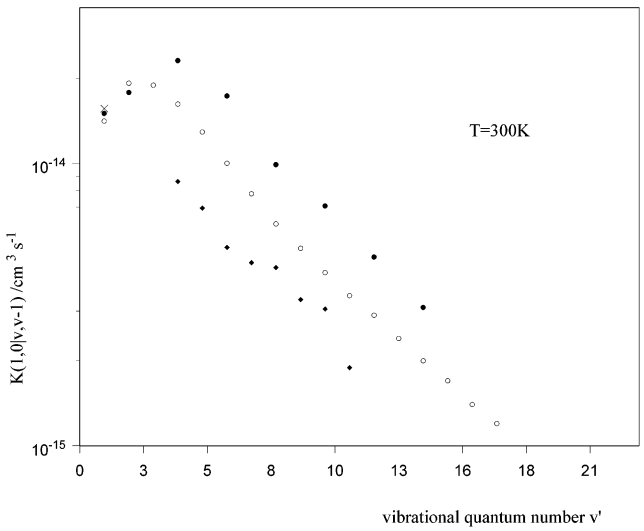

Figure 5. Exothermic rate constants for the process $N_2(v = 1) + CO(v' - 1) \rightarrow N_2(v = 0) + CO(v')$ reported as a function of the vibrational quantum number v' at $T = 300$ K. Comparison is shown between our results (●) and the experimental data of Hancock and Smith[27] (♦) and Allen and Simpson[16] (×). Open circles are the analytical rates from eq A5 of the Appendix.

TABLE 4: Endothermic Rate Constants for the Process $N_2(v = 0) + CO(v' = 8) \rightarrow N_2(v = 1) + CO(v' = 7)$

T/K	expt (ref 21)	Pot I	Pot II	Pot III	Pot II (ref 2)
100		5.75(−18)	2.43(−17)	3.02(−17)	3.39(−18)
200		3.32(−16)	5.99(−16)	6.94(−16)	1.97(−16)
300	7.20(−16)	1.67(−15)	2.74(−15)	3.17(−15)	1.30(−15)
500		1.24(−14)	1.48(−14)	1.76(−14)	9.45(−15)
1000		8.74(−14)	9.22(−14)	1.16(−13)	7.72(−14)
2000		3.61(−13)	3.58(−13)	4.44(−13)	
3000		6.66(−13)	6.62(−13)	7.71(−13)	

fact, the semiclassical rates $K(1,0|v' - 1, v') > 1$, are overestimated, a behavior also observed in the previous work.[2] The origin of such discrepancy is not evident and open to question, considering that we do not expect the dynamics of the first vibrationally excited states of CO to be significantly different to the relaxation dynamics of the $v = 1$ state (the vibrational anharmonicity is treated exactly in the dynamical model assumed in the present calculations). On the other hand, a satisfactory agreement between experiment and theory was reached[28] for similar transitions in vibrationally excited CO but in CO−CO collisions: $CO(v) + CO(v = 0) \rightarrow CO(v + 1) + CO(v = 1)$.

The analytical rate constants reported in Figure 5 obtained from approximate first order theory (see the Appendix) are also overestimated when compared with the experimental data. A different choice for the interaction potential would not led to better results.

In Table 4, we have reported the rate constant for the transition: $N2(v = 1) + CO(v' = 8) \rightarrow N_2(v = 0) + CO(v' = 7)$ calculated assuming Pots II and III within the semiclassical coupled state method. It turns out that the semiclassical rate constants are again overestimated.

As second objective of this work, that is the investigation on the relaxation of vibrationally excited states relevant to CO/N2 low-temperature plasmas, we made calculations for processes 2. In Table 5 there are reported the rate constants for the symmetric processes

$$N_2(v = 28) + CO(v') \rightarrow N_2(v = 28 - \Delta v) + CO(v' + \Delta v), \quad \Delta v = 1, 2;\ v' = 18-30 \quad (22)$$

In this table, a comparison is also made with the rate constants calculated in the harmonic oscillator approximation.[2] For all of the considered transitions, the updated rate constants are smaller than those previously calculated. The largest discrepancies are observed for the two quantum transitions, more than 2 orders of magnitude for the transition with the largest energy mismatch. The use of the new set of rate constants could have important consequences on the relaxation kinetics of CO in the high-lying vibrational levels. The dependence of the V−V rate constant ($K(28,28 - \Delta v|v', v' + \Delta v)$) for N_2 in the given $v = 28$ vibrational state as a function of the vibrational quantum number v' of CO in closest resonance with N_2 gives rice to the well-known "resonant" excitation curve shown in Figure 6 often used in kinetic modeling. The behaviors of the resonant curves for V−V enegy exchanges and some aspects relevant to the use of analytical first-order based collisional theory to fit these curves are discussed in refs 28 and 29.

A large impact of the vibrational anharmonicity is expected for multiquantum dissymmetric transitions in N_2−CO collisions with CO in vibrationally excited states. We have investigated the following near-resonance asymmetric processes:

$$N_2(v = 0) + CO(v') \rightarrow N_2(v = 1) + CO(v' - 2), \quad v' > 32 \quad (23)$$

The corresponding rate constants, presented in Figure 7 for $T = 100$ and 500 K, are quite sizable and reach the values up to 4×10^{-13} cm^3 s^{-1}. The role of such processes in vibrational kinetics of highly excited CO molecules may be very important for vibrational kinetics modeling in CO:N_2 mixtures[30] and even greater than the role of analogous recently studied asymmetric processes:[6] $CO(v) + CO(v = 0) \rightarrow CO(v - 2) + CO(v = 1)$ and this because the discussed CO−N_2 processes exert strong influence at lower levels. It is also important for understanding situation with competition of V−V and V−T processes at high vibrational levels. In any case, the obtained rate constants for dissymmetric V−V exchanges of highly excited CO with nonexcited N_2 are needed in experimental verification. The calculations performed for analogous asymmetric three-quantum exchange processes $CO(v') + N_2(v = 0) \rightarrow CO(v' - 3) + N_2(v = 2)$, $v' = 22 \div 28$, led to near-resonance rate constant values less than 2.5×10^{-17} cm^3 s^{-1} and consequently their role for vibrational kinetics modeling will be not so significant.

5. Final Remarks

Semiclassical calculations of the V−V relaxation between low-lying and vibrationally excited states of N_2 and CO in N_2−CO collisions were performed using different updated interaction potentials obtained as the sum of ab initio determined SR and long-range dispersion attractions. For the $K(1,0|0,1)$ rate constant, the best agreement (within 10%) between the theoretical and the experimental data[16,22] in the low and thermal temperature range, $T = 80-600$ K, was reached using the "base" Pot I of ref 8. The inclusion of the higher order dispersion and multipole expansion terms does not improve the performance of the potential surface: it turns out that the rate constants, besides of being very sensitive to the choice of the octopole parameters, are overestimated. Considering also the superiority of this ab initio potential with respect to the previously proposed semiempirical potential to well describe the vibrational energy exchange in the low collisional energy regime, the calculations were then extended and a set of rate constants for excited CO and N_2 molecules have also been recalculated. It is found that the

TABLE 5: Rate Constants for Single and Two-Quantum Vibrational Energy Exchanges in Collisions between N_2 and CO: $N_2(v = 28) + CO(v_1) \rightarrow N_2(v' = v - \Delta v) + CO(v_1' = v_1 + \Delta v) + \Delta E$

(v,v')	(v_1,v_1')	$T = 200$K	300 K	500 K	700 K	1000 K	ΔE(cm^{-1})
(28,27)	(18,19)	4.46(−12)[a]	7.49(−12)	1.11(−11)	1.44(−11)	1.79(−11)	126.44
(28,26)	(18,20)	7.72(−14)	1.36(−13)	2.20(−13)	3.24(−13)	4.62(−13)	198.63
(28,27)	(20,21)	1.52(−11)	1.86(−11)	2.23(−11)	3.33(−11)	2.53(−11)	77.86
		2.58(−11)[b]					
(28,26)	(20,22)	6.30(−13)	5.99(−13)	6.19(−13)	6.57(−13)	8.54(−13)	105.11
		8.00(−13) [b]					
(28,27)	(22,23)	3.15(−11)	3.04(−11)	2.87(−11)	2.90(−11)	3.13(−11)	25.42
(28,26)	(22,24)	2.76(−12)	2.00(−12)	1.41(−12)	1.25(−12)	1.39(−12)	3.16
(28,27)	(24,25)	3.10(−11)	3.06(−11)	3.11(−11)	3.22(−11)	3.46(−11)	12.82
		4.65(−11) [b]					
(28,26)	(24,26)	6.88(−13)	6.96(−13)	8.57(−13)	1.10(−12)	1.51(−12)	75.53
		4.32(−12) [b]					
(28,27)	(28,29)	9.33(−12)	1.56(−11)	2.44(−11)	3.02(−11)	3.77(−11)	100.55
		3.30(−11)[b]					
(28,26)	(28,30)	1.00(−13)	2.61(−13)	6.50(−13)	1.03(−12)	1.62(−12)	250.24
		7.30(−12)[b]					
(28,27)	(30,31)	3.07(−12)	6.12(−12)	1.27(−11)	1.85(−11)	2.60(−11)	143.31
		2.30(−11)[b]					
(28,26)	(30,32)	1.80(−14)	5.80(−14)	2.15(−13)	4.58(−13)	9.11(−13)	335.39
		2.15(−12)[b]					

[a] This work. [b] From Figure 12 of ref 2.

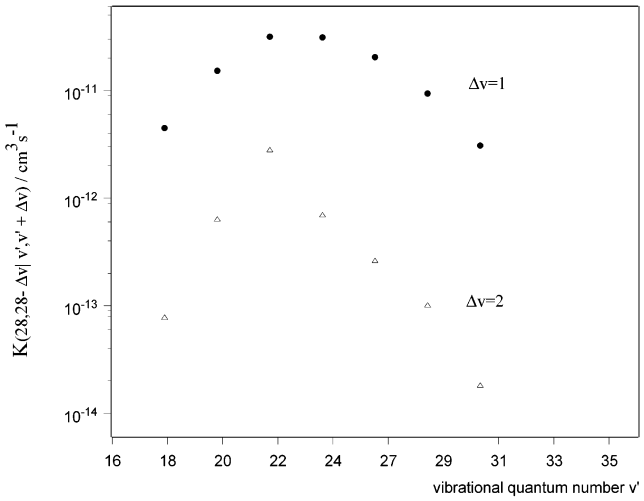

Figure 6. Theoretical rate constants for single and two-quantum vibrational exchanges in the processes $N_2(v = 28) + CO(v') \rightarrow N_2(v = v - \Delta v) + CO(v' + \Delta v)$ shown at $T = 200$ K and v' in the range $18 \div 30$.

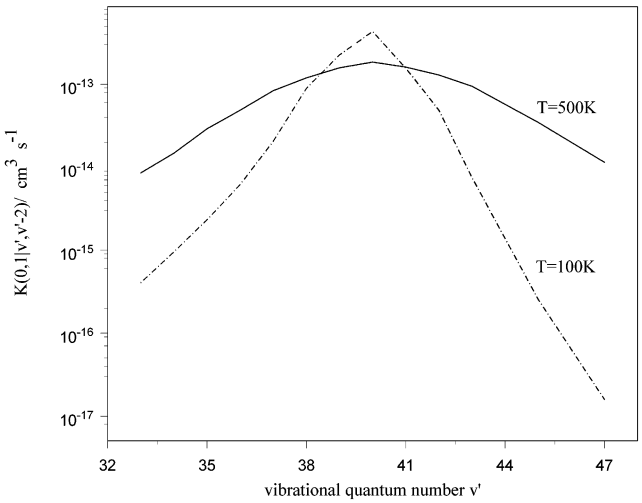

Figure 7. Semiclassical rate constants for the processes $N_2(v = 0) + CO(v') \rightarrow N_2(v = 1) + CO(v' - 2)$ are reported versus v at $T = 100$ and 500 K.

introduction of the new potential within the coupled state expansion method led to remarkable corrections of multiquantum rate constants calculated for the same processes in previous studies. The calculated rate constants for near resonance asymmetric processes: $CO(v') + N_2(v = 0) \rightarrow CO(v' - 2) + N_2(v = 1)$, $v > 32$, are quite sizable (so as for analogous processes $N_2(v = 40) + CO(v') \rightarrow N_2(v = 38) + CO(v' + 1)$, $v = 0, 4$) and should be taken into account in vibrational kinetics modeling of overtone CO laser. However, because the dynamics of highly vibrationally excited molecules can be different than the relaxation of the ground and the first excited vibrational state, the calculated rate constants for single and multiquantum exchanges in the region of high v should be validated on an experimental ground only.

Discrepancies are observed in the high-temperature region, $T \geq 2000$ K, between the calculated $K(1,0|0,1)$ rate constant and the data obtained in shock tube experiments, but no attempt was made to fit the short-range potential parameters to the experimental data. Although this disagreement is somehow expected due to the wide temperature range explored (80−4000 K), quite surprisingly, discrepancies still persist for the relaxation of the low-lying levels of CO at $T = 300$ K. As mentioned in the previous section, it is interesting to note that a reasonable agreement was obtained for similar transitions in CO−CO collisions between theory and the experimental data available for this system.

Therefore, on the light of the analysis presented in this work on the vibrational relaxation in N_2−CO collisions, more experimental investigations on the relaxation of vibrationally excited CO are needed as well as theoretical improvements to a better characterization of the N_2−CO interaction potential.

Acknowledgment. The authors thank Prof. A. Napartovich for fruitful discussions and collaboration. This work is part of the project "Dynamics and kinetics of elementary processes in hypersonic flows" supported by the Italian Space Agency (ASI).

6. Appendix

We used for analytical calculations the modified Schwartz−Slawsky−Herzfeld (SSH) theory expressions analogous to that as in ref 31. In this case, both kinds of interactions, short-range

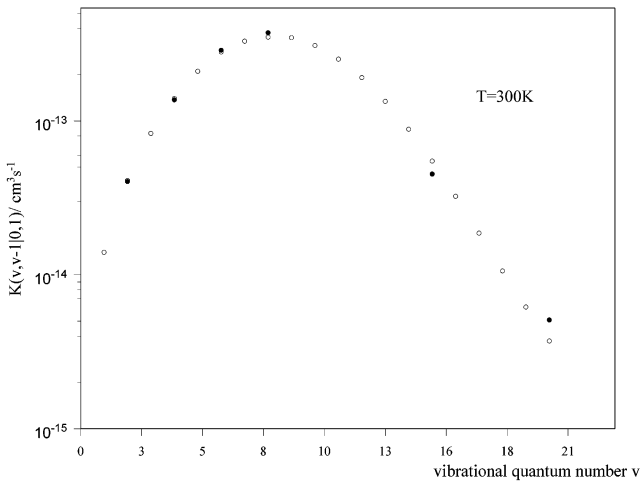

Figure 8. Rate constants for the processes $N_2(v) + CO(v' = 0) \rightarrow N_2(v - 1) + CO(v' = 1)$. The semiclassical rates are indicated by full circles, and the analytical rates are shown by open circles. The gas temperature is $T = 300$ K.

and long-range, were taken into account. A part due to the short-range interactions was described by the formula

$$^{SR}K(v',v'+1|v,v-1) = azT\frac{v}{(1-v\delta)}\frac{(v'+1)}{(1-(v'+1)\delta)}\exp\left(\frac{\Delta E}{2T}\right) f(y(\Delta E,T))\, F \quad \text{(A.1)}$$

where $a = 6.61 \times 10^{-8}\ K^{-1}$, $z = (\pi\sigma^2/4)V_M$ is gas kinetic collision rate constant, V_M is the average relative translation velocity, $(\pi\sigma^2/4)$ is the gas kinetic collision cross section, and $f(y)$ is an adiabatic factor

$$f(y) = 8(\pi/3)^{1/2} y^{7/2} \exp(-3y^{2/3}) \qquad y \geq 21.622 \quad \text{(A2)}$$

$$f(y) = 0.5\exp(-2y/3)(3 - \exp(-2y/3)) \qquad y < 21.622 \quad \text{(A3)}$$

The factor F accounts for attractive part of intermolecular interaction. Simple SSH theory assumes an exponential repulsive interaction potential between the colliding molecules. To account for the attractive well caused by dispersion interactions, a multiplicative factor was used as in ref 32.

For description of the long-range interactions, the next analytical approximation was used

$$^{LR}K(v',v'+1|v,v-1) = bz\frac{1}{T}\frac{v}{1-v\delta}|\langle v'+1|q|v'\rangle|^2 \exp\left(\frac{\Delta E}{2T}\right)\exp\left(-\frac{\Delta E^2}{Tc}\right) \quad \text{(A4)}$$

here $b = 4 \times 10^{-2}K$, $c = 145K$, $|\langle v' + 1|q|v'\rangle$ is the matrix element of quadruple moment of a nitrogen molecule. The total V−V′ exchange rate coefficient was calculated according to the formula:

$$K(v',v'+1|v,v-1) = {}^{SR}K(v',v'+1|v,v-1) + {}^{LR}K(v',v'+1|v,v-1) \quad \text{(A5)}$$

Empirical coefficients a, b, and c were determined[33] by means of fitting procedure to the experimental rate constants $K(0,1|1,0)$ for the vibrational deactivation of $CO(v = 1)$ and its isotopic variants with $N_2(v = 0)$.[16]

The results obtained with these analytical expressions for exothermic processes 21 are reported in Figure 5 and compared with semiclassical rates and experimental data. It is seen that the analytical rate constants are between the experimental and the ab initio semiclassical rates with the maximum shifted downward to $v' = 3$.

To make more clear the v-scaling behavior of analytical rates compared to ab initio results, we also performed calculations for processes

$$N_2(v) + CO(v' = 0) \rightarrow N_2(v-1) + CO(v' = 1) \quad v = 1,20 \quad \text{(A6)}$$

at $T = 300$ K. The corresponding v dependences reported in Figure 8 demonstrate a good agreement between the analytical and the ab initio rates. The modified SSH-based expressions may be used for these processes.

References and Notes

(1) Basov, N. G.; Hager, G. D.; Ionin, A. A.; et al. *IEEE J. QE* **2000**, *36*, 810.
(2) Cacciatore, M.; Capitelli, M.; Billing, G. D. *Chem. Phys.* **1989**, *89*, 17.
(3) Billing, G. D. *Chem. Phys.* **1980**, *50*, 165.
(4) Balakrishnan, N.; Billing, G. D. *Chem. Phys.* **1996**, *204*, 77.
(5) Coletti, C.; Billing, G. D. *J. Chem. Phys.* **1999**, *111*, 3891.
(6) Coletti, C.; Billing, G. D. *J. Chem. Phys.* **2000**, *113*, 4869.
(7) Billing, G. D. *Chem. Phys.* **1978**, *30*, 387.
(8) Ling, M. S. H.; Rigby, M. *Mol. Phys.* **1984**, *51*, 855.
(9) Billingsley, F. P.; Krauss, M. *J. Chem. Phys.* **1974**, *60*, 2767.
(10) Buckingham, A. D.; Graham, C.; Williams, J. H. *Mol. Phys.* **1983**, *49*, 703.
(11) Reuter, D.; Jennings, D. E. *J. Mol. Spectrosc.* **1986**, *115*, 294.
(12) Langhoff, S. R.; Baushlicher, C. W. *J. Chem. Phys.* **1995**, *102*, 5220.
(13) Yong, L. A.; Eachus, W. J. *J. Chem. Phys.* **1966**, *44*, 4195.
(14) Parker, G. A.; Pack, R. T. *J. Chem. Phys.* **1976**, *64*, 2010.
(15) Billing, G. D. *Comput. Phys. Rept.* **1984**, *1*, 237.
(16) Allen, D. S.; Simpson, C. J. S. M. *Chem. Phys.* **1980**, *45*, 203.
(17) Tang, K. T.; Toennies, J. P. *J. Chem. Phys.* **1984**, *80*, 3726.
(18) Rijks, W.; Wormer, P. E. S. *J. Chem. Phys.* **1989**, *90*, 6507.
(19) Poulsen, L.; Billing, G. D. *Chem. Phys.* **1984**, *89*, 219.
(20) Meerts, W. I. *Chem. Phys.* **1977**, *22*, 319.
(21) Spelsberg, D.; Meyer, W. *J. Chem. Phys.* **1999**, *111*, 9618.
(22) Mastrocinque, G.; Chakroun, A.; Doyennette, L.; Gueguen, H.; Margottin-Maclou, M.; Henry, L. *Chem. Phys. Lett.* **1976**, *39*, 347.
(23) Starr, D. F.; Hancock, J. K.; Green, W. H. *J. Chem. Phys.* **1974**, *61*, 5421.
(24) McLaren, T. I.; Appleton, J. P. *Proc. 8th Int. Shock Symposium*; Stollery, J. I.; Gaydon, A. G., Owen, P. R., Eds.; Chapman and Hall: London, 1971.
(25) Sato, Y.; Tsuchiya, S.; Kwiatani, K. *J. Chem. Phys.* **1969**, *50*, 1911.
(26) von Rosenberg, C. W.; Bray, K. C. N.; Pratt, N. H. *J. Chem. Phys.* **1972**, *56*, 3230.
(27) Hancock, G.; Smith, I. W. M. *Appl. Opt.* **1971**, *10*, 1827.
(28) Cacciatore, M.; Billing, G. D. *Chem. Phys.* **1981**, *58*, 395.
(29) Cacciatore, M. In *Molecular Physics and Hypersonic Flows*; Capitelli., M., Ed.; Kluwer Academic Publishers: Norwell, MA, 1996; pp 21−34.
(30) Cacciatore, M.; Kurnosov, A.; Napartovich, A. *Proc. Int. Conf. ICPEAC*; Santa Fe, 2001; p 596.
(31) Smith, N. S.; Hassan, H. A. *AIAA J.* **1976**, *14*, 374.
(32) Shin, H. K.*J. Chem. Phys.* **1965**, *42*, 59.
(33) Ionin, A. A.; Kasakevich, V. S. et al. Preprint Lebedev Physical Institute (in Russian) N.232, Moscow, 1982.